

# DARK CURRENT MEASUREMENTS AT THE PITZ RF GUN

I. Bohnet, J. H. Han\*, M. Krasilnikov, F. Stephan, DESY Zeuthen, 15738 Zeuthen, Germany  
K. Flöttmann, DESY Hamburg, 22603 Hamburg, Germany

## Abstract

For photocathode rf guns with electric fields of more than 40 MV/m at the photocathode and with an rf pulse length of 100  $\mu$ s or more, the amount of dark current might be comparable with the photoelectron beam. At the photoinjector test facility at DESY Zeuthen (PITZ) the dark current was measured with a Faraday cup for various settings of the solenoid fields at the rf gun. We discuss the dark current behavior for different photocathodes. Experimental results are compared with simulations.

## INTRODUCTION

The photoinjector test facility at DESY Zeuthen (PITZ) has been developed with the aim to achieve high quality electron beams and study their characteristics for future applications at free electron lasers and linear colliders. At PITZ, the photocathode rf gun is operated with a rf frequency of 1.3 GHz, a maximum electric field of 41 MV/m at the photocathode, a maximum rf pulse length of 900  $\mu$ s, and a maximum repetition rate of 10 Hz.

Due to the high electric field and the long field emission time, the amount of dark current might be comparable to the photoelectron beam. Such a strong dark current degrades the electron beam quality and impairs emittance and energy spread measurements. More seriously, a large dark current is a severe hazard for a superconducting linac as it may produce X-rays, cryogenic losses, and radioactive activation. In the following paper, the generation of dark current and its properties are studied with measurements and simulation.

## FIELD EMISSION AT THE RF GUN

The field emission of electrons is the main source of dark current. The field emission current at the rf gun can be parameterized in terms of the modified Fowler-Nordheim equation [1]

$$I_F = \frac{1.54 \times 10^{-6} \times 10^{4.52\phi^{-0.5}} A_e (\beta E)^2}{\phi} \times \exp\left(-\frac{6.53 \times 10^9 \phi^{1.5}}{\beta E}\right), \quad (1)$$

where  $E$  is the surface electric field in V/m,  $\phi$  is the work function of the emitting material in eV,  $\beta$  is a field enhancement factor, and  $A_e$  is the effective emitting area.

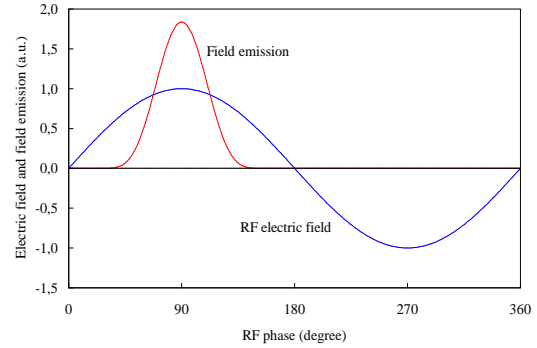


Figure 1: Intensity distribution of the field emission and the strength of the rf electric field for an rf cycle. The field emission curve was computed from the modified Fowler-Nordheim equation (Eq. 1) with an sinusoidal rf field and the typical  $\beta$  and  $\phi$  values of 200 and 4.5 eV, respectively.

Figure 1 shows that the field emission is concentrated on the maximum electric field region of an rf cycle. Therefore, the field emitted electrons produced on the cathode are preferably accelerated in forward direction by the rf electric field.

At the rf gun, the field emitted electrons from other sources, like the iris or the entrance to the coupler, cannot follow the downstream component of the accelerating field, because these electrons are not synchronized to the accelerating rf electric field. However, they are able to heat up the cavity surface and may create secondary electrons.

The average field emission current during one rf cycle is described as [1]

$$\bar{I}_F = \frac{5.7 \times 10^{-12} \times 10^{4.52\phi^{-0.5}} A_e (\beta E_0)^{2.5}}{\phi^{1.75}} \times \exp\left(-\frac{6.53 \times 10^9 \phi^{1.5}}{\beta E_0}\right), \quad (2)$$

where  $E_0$  is the amplitude of the sinusoidal macroscopic surface field in V/m.

## MEASUREMENTS

The experimental setup is shown in Fig. 2. A molybdenum (Mo) cathode is a circle with a radius of 8 mm and a cesium telluride ( $\text{Cs}_2\text{Te}$ ) cathode is a circle with a radius of 4 mm on a Mo substrate which has the same geometry as the Mo cathode except for the  $\text{Cs}_2\text{Te}$  coating. The

\*jhhan@ifh.de

Mo cathode is used for conditioning of the rf gun and the Cs<sub>2</sub>Te cathode is used to produce the photoelectron beam in normal operation. A main solenoid is located at 28 cm downstream of the cathode. The rf frequency is 1.3 GHz and the rf power is transferred into the gun cavity through a coaxial coupler. A laser with a wavelength of 262 nm produces the electron beam with a pulse length of 8 ps. The bunch repetition rate of the laser pulse train is 1 MHz.

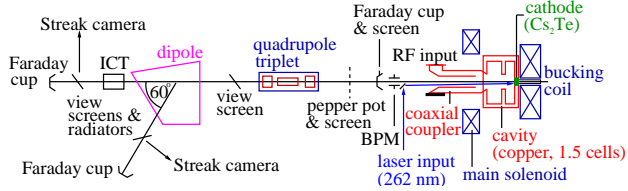


Figure 2: Schematic view of the gun and diagnostic sections.

Dark current signals were obtained with a removable Faraday cup which is located about 76 cm downstream of the cathode. The average dark current during an rf cycle was measured at the end of the rf pulse. Using the spectrometer dipole it was determined that the dark current has nearly the same momentum as the electron beam, which means the major part of the dark current is generated near the photocathode.

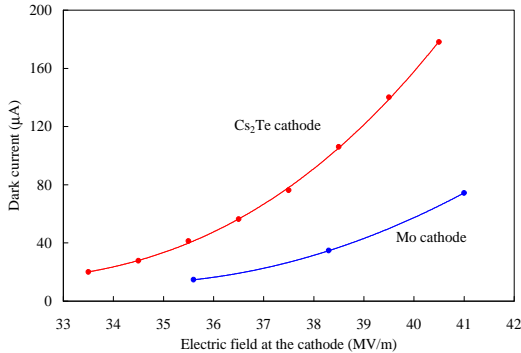


Figure 3: Maximum dark current measured as a function of the electric field at the cathode.

The dark current is higher for the Cs<sub>2</sub>Te cathode than for the Mo cathode (Fig. 3) and the magnetic field dependencies are different for the Cs<sub>2</sub>Te and Mo cathodes (Fig. 4, 5).

The amount of dark current reaching the Faraday cup depends on the strength of the magnetic field of the main solenoid. This is related to the current by  $B_0$  [mT] =  $0.6 \times I_{Main}$  [A]. The iris in the gun, the beam tube, the entrance to the coupler, and the mirror reflecting the laser beam onto the photocathode play a role as apertures for the dark current beam. A guiding force provided by the main solenoid field and the rf field guides the dark current through these apertures. The focusing behavior (see Fig. 4 and 5) of the dark current shows that the dark current has an energy comparable to the electron beam and starts near the

cathode because the best focusing condition on the Faraday cup of the electron beam with low charge is about 250 A at 40 MV/m accelerating electric field.

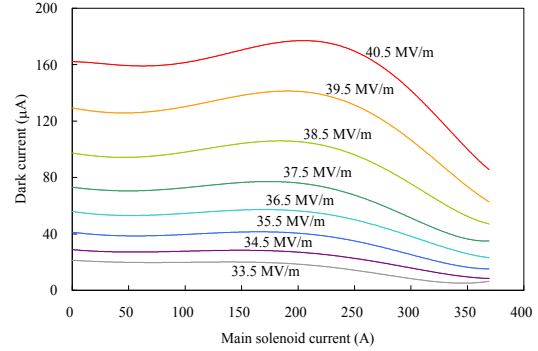


Figure 4: Dark current as a function of the main solenoid field for a Cs<sub>2</sub>Te cathode at different rf fields.

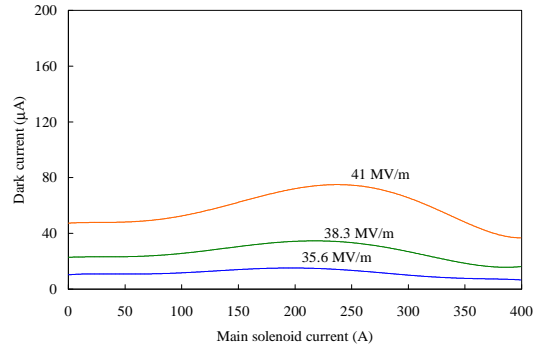


Figure 5: Dark current as a function of the main solenoid field for a Mo cathode at different rf fields.

With an rf electric field of 40.5 MV/m and a main solenoid current of 200 A, the dark current for a Cs<sub>2</sub>Te cathode is about 180 μA. According to simulation results, about 50 % of the field emitted electrons from a 4 mm rms area at the cathode reach the Faraday cup. This means the amount of dark current generated near the Cs<sub>2</sub>Te cathode is comparable to the electron beam in normal operation.

The field enhancement factor  $\beta$  was found from the Eq. 2 [1]

$$\frac{d(\log_{10} I_F / E^{2.5})}{d(1/E)} = -\frac{2.84 \times 10^9 \phi^{1.5}}{\beta}. \quad (3)$$

In this calculation, the work function  $\phi$  was assumed to be 4.75 eV [2] for the Cs<sub>2</sub>Te cathode and 4.2 eV for Mo cathode. The calculated field enhancement factors for the Cs<sub>2</sub>Te and Mo cathodes are 220 and 164, respectively. The effective emitting areas were calculated to be  $1.1 \times 10^{-15} \text{ m}^2$  and  $1.2 \times 10^{-15} \text{ m}^2$  for the Cs<sub>2</sub>Te and Mo cathodes, respectively.

In normal operation, the bucking solenoid is used to compensate the longitudinal magnetic field produced by

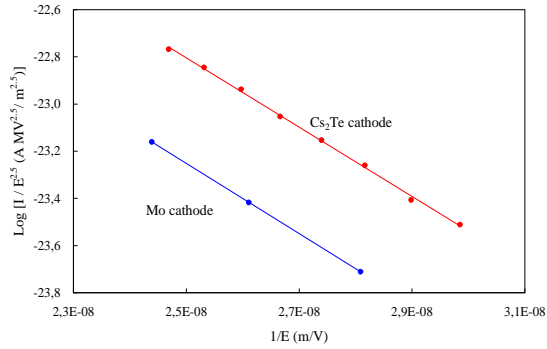


Figure 6: Fowler-Nordheim plots to find enhancement factors and effective field emission areas for each cathodes.

the main solenoid at the cathode. But Fig. 7 shows that the bucking solenoid can also affect the dark current behavior for the  $\text{Cs}_2\text{Te}$  cathode. Such a bucking solenoid dependency of the dark current was not found for the Mo cathode. The relation between the main and the bucking solenoid currents to compensate the magnetic field at the cathode is  $I_{\text{Bucking}} [\text{A}] = 0.0846 \times I_{\text{Main}} [\text{A}]$  for the present experimental setup. The magnetic field at the cathode has no influence on electron field emission (see Eq. 1). The magnetic field dependence of the dark current is possibly caused by secondary electron emission.

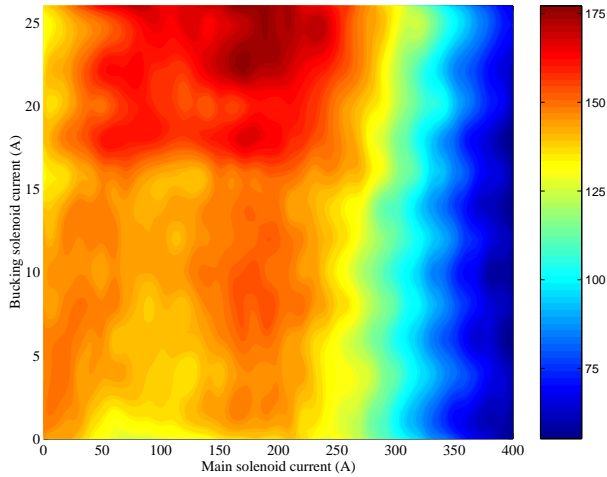


Figure 7: Contour plot of the dark current at 40 MV/m for the  $\text{Cs}_2\text{Te}$  cathode with the combination of the main solenoid and the bucking solenoid currents.

A particle tracking code (ASTRA) [3] was used to simulate the dark current. In this simulation, the dark current source was assumed to be the cathode itself and the surrounding area, a Gaussian distribution with  $\sigma = 4 \text{ mm}$  was taken. The time structure of the field emission current has been derived from Fig. 1. A Gaussian distribution in the rf phase was assumed with a center value of  $90^\circ$  and a variance of  $20^\circ$ . The simulation result using ASTRA without secondary electron emission is similar to the dark current

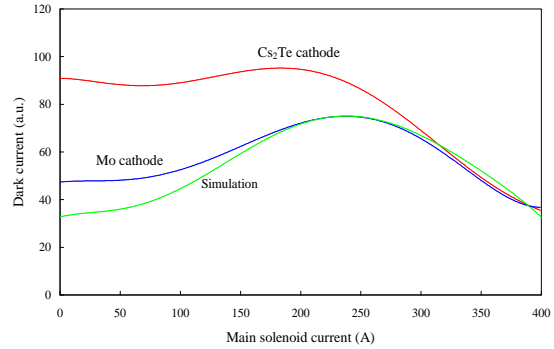


Figure 8: Comparison of dark current measurements for the  $\text{Cs}_2\text{Te}$  and Mo cathodes with the ASTRA simulation. Measurements are normalized at the high magnetic field region.

behavior for the Mo cathode (see Fig. 8). The study on the dark current behavior for the  $\text{Cs}_2\text{Te}$  cathode is ongoing considering secondary electron emission.

## SUMMARY

The main source of the dark current at the rf gun is found experimentally and in simulations to be the cathode and the surrounding area. The magnetic field dependence of the dark current is quite different for the  $\text{Cs}_2\text{Te}$  and Mo cathodes. The simulation using ASTRA without secondary electron emission is similar to the dark current behavior for the Mo cathode. The dark current behavior for the  $\text{Cs}_2\text{Te}$  cathode is possibly caused by secondary electron emissions, which will be studied in future.

## REFERENCES

- [1] J. W. Wang and G. A. Loew, "Field emission and rf breakdown in high-gradient room-temperature linac structures," SLAC-PUB-7684, 1997.
- [2] S. H. Kong, et. al., "Cesium telluride photocathodes," J. Appl. Phys. **77**, 6031 (1995).
- [3] K. Flöttmann, A Space Charge Tracking Algorithm (ASTRA), <http://www.desy.de/~mpyfb/>.